Journal Name

ARTICLE TYPE

Cite this: DOI: 10.1039/xxxxxxxxxx

Received Date
Accepted Date

DOI: 10.1039/xxxxxxxxxx

www.rsc.org/journalname

Reaction processes among self-propelled particles

Fernando Peruani,*[a] Gustavo J. Sibona[b‡]

We study a system of self-propelled disks that perform run-and-tumble motion, where particles can adopt more than one internal state. One of those internal states can be transmitted to other particle if the particle carrying this state maintains physical contact with another particle for a finite period of time. We refer to this process as a *reaction process* and to the different internal states as *particle species* making an analogy to chemical reactions. The studied system may fall into an absorbing phase, where due to the disappearance of one of the particle species no further reaction can occur, or remain in an active phase where particles constantly react. Combining individual-based simulations and mean-field arguments, we study the dependency of the equilibrium densities of particle species with motility parameters, specifically the active speed v_0 and tumbling frequency λ. We find that the equilibrium densities of particle species exhibit two very distinct, non-trivial scaling regimes with v_0 and λ depending on whether the system is in the so-called ballistic or diffusive regime. Our mean-field estimates lead to an effective renormalization of reaction rates that allow building the phase-diagram v_0–λ that separates the absorbing and active phase. We find an excellent agreement between numerical simulations and estimates. This study is a necessary step to an understanding of phase transitions into an absorbing state in active systems and sheds light on the spreading of information/signaling among moving elements.

1 Introduction

Systems of self-propelled particles are found in biology across scales, from bacteria[1–3] to animal groups[4,5]. There exist also man-made self-propelled systems such as chemically driven particles[6,7], vibration-driven disks[8] and various types of active rollers[9,10] among many other examples. Requiring particles to convert energy into work to self-propel in dissipative media, self-propelled particle systems are intrinsically nonequilibrium systems[11–13]. Given the nonequilibrium nature of these systems, self-propelled particle systems display a large variety of phenomena that cannot be found in equilibrium systems as for instance the spontaneous, self-organized emergence of long-range order in the form of large-scale collective motion in two-dimensions that was initially found in models[14–16] and later confirmed to exist in real-world systems[8,9,17]. It is worth noting that it was recently observed that the presence of spatial heterogeneities such as imperfections on the substrate where particles move – typically present in real systems – prevents the emergence of large-scale collective motion[18,19]. Not surprisingly, most experimental self-propelled systems do not display global collective motion and particle motion remains diffusive at large time scales[1–3,6]. However, even in the absence of global order, the self-propulsion of active particles induces remarkable nonequilibrium features such as non-equilibrium clustering[3,20–22], nonequilibrium phase-separation[23–25], and enhanced sedimentation[26].

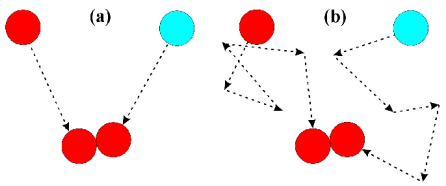

Fig. 1 The figure shows two scenarios [(a) aand (b)] where a red agent "activates" a blue one agent after an encounter/collision among the two agents. In (a) particles move in straight trajectories (ballistic regime) in between collisions, while in (b) particles perform several turns (diffusive regime). Note that in an over-damped dynamics, a collision event lasts a finite time. Importantly, the steady state densities of particles species (e.g. density of red and blue agents) depend on the motility parameters of the active particles, namely active speed v_0 and tumbfling frequency λ. For movies, see SI.

Here, we aim at studying the spreading of information/signaling among actively moving units that do not display large-scale order. With this goal in mind, we analyze a system of self-propelled disks that perform run-and-tumble motion, where particles can adopt more than one internal state, see Fig. 1. One

[a] *Université Côte d' Azur, Laboratoire J.A. Dieudonné, UMR CNRS 7351, Parc Valrose, F-06108 Nice Cedex 02, France; E-mail: peruani@unice.fr*
[b] *CONICET and Fa.M.A.F., Universidad Nacional de Córdoba, Córdoba, Argentina; E-mail: sibona@famaf.unc.edu.ar*

† Electronic Supplementary Information (ESI) available: [details of any supplementary information available should be included here]. See DOI: 10.1039/b000000x/

of those internal states can be transmitted to other disk if the disk carrying this state maintains physical contact with another disk for a finite period of time. Making an analogy to chemical reaction, we refer to this process as a reaction process and say that particles in the same internal state belong to the same particle species. The objective of current study is to understand how the steady state densities of particle species depend on the motility parameters of the self-propelled disks – shedding light on the way information spreads in active systems – in the context of reaction processes with an absorbing state. It is worth recalling that phase transitions into absorbing states is one of the fundamental problems in non-equilibrium statistical physics[27–29]. Here we intend to make a first step to understand how activity in the form of self-propulsion affects this classical problem of nonequilibrium statistical physics. It is important to stress that the understanding of the role of particle motion in reaction processes is key for a large number of applications beyond the context of active systems. For instance, it is well-known that the average concentration of (non self-propelled) chemical elements depends on how the system is stirred[30,31]. In ecology, the mobility of individuals affects the level of biodiversity[32,33]. In epidemics, it has been shown that the motion of individuals impacts the statistics of disease outbreaks[34–39]. In microbiology, the spreading of pathogens[40,41] and the spatial distribution of gene expressions and cell types[32,42] are known to be correlated to cell motility. Finally, in the context of social dynamics, it has been shown that moving-agent models can be used as a proxy to mimic realistic social dynamics[43], which paved the way to study opinion dynamics in moving-agent systems[44,45]. In summary, studying how the spreading of information/signaling is affected by the motility parameters of active particles is a fundamental problem in active matter – and in the broad context of nonequilirbium statistical mechanics – which may have important implications for a large number of applications.

2 Model definition

2.1 Particle motion

We consider, as in[46], a two-dimensional system of N self-propelled disks moving in a box of linear size L with periodic boundary conditions. The equation of motion of the i-th disk is given by:

$$\dot{\mathbf{x}}_i(t) \quad = \quad v_0\mathbf{v}(\theta_i) - \sum_{j\neq i}\nabla U(\mathbf{x}_i(t),\mathbf{x}_j(t))\,, \tag{1}$$

where $\mathbf{x}_i(t)$ is the position of the particle, v_0 is the active speed, $\mathbf{v}(\theta_i) = (\cos(\theta_i),\sin(\theta_i))$ with θ_i an angle that denotes the propulsion direction. The propulsion direction θ_i obeys a classical Poisson process: at rate λ – which we refer to as tumbling frequency – a new angle is selected from the interval $[0,2\pi)$. This defines a classical run-and-tumble process[47,48], whose distribution $p(\theta_i,t)$ obeys $\partial_t p(\theta_i,t) = -\lambda\, p(\theta_i,t) + \int d\theta' T(\theta'\to\theta_i)p(\theta',t)$, where $T(\theta'\to\theta_i) = \frac{\lambda}{2\pi}$ is the transition probability from $\theta'\to\theta_i$. Note that $p(\theta_i,t\to\infty) = \frac{1}{2\pi}$ and the particle stays in a given direction a characteristic time λ^{-1}. In between turnings, particles interact through a soft-core potential U, which penalizes particle overlapping. Specifically, we implement a two-body repulsive potential, which depends on the distance between the center of mass of the two disks as follows:

$$U(\mathbf{x},\mathbf{x}') = \begin{cases} a(v_0)\left[\left(\frac{|\mathbf{x}-\mathbf{x}'|}{2r}\right)^{-b} - 1\right] & \text{if } |\mathbf{x}-\mathbf{x}'| < 2r \\ \\ 0 & \text{if } |\mathbf{x}-\mathbf{x}'| \geq 2r \end{cases} \tag{2}$$

where r is the radius of the disks, b is a constant, and $a(v_0)$ is a linear function of v_0, $a(v_0) = c_1 + c_0 v_0$ such that the maximum overlapping area between two agents is independent of v_0. By appropriately choosing the units of a, we have absorbed the mobility constant in such that ∇U has units of speed instead of force. Note that b controls how soft/hard is the potential U, becoming increasingly harder as b is increased. In the following we fix the parameters $r = 1$, $c_0 = 1.62$ (in units of distance), $c_1 = 10^{-4}$ (in units of speed squared), $b = 1$, and the density to $d_0 = N/L^2 = 0.045$ ensuring that for the explored range of v_0 and λ the system remains in the gas phase. Under these conditions, the motion of the self-propelled disks can be approximated by Fürth's formula:

$$\langle \mathbf{x}^2(t)\rangle \quad \simeq \quad 2\frac{v_0^2}{\lambda^2}(\lambda t - 1 + e^{-\lambda t})\,, \tag{3}$$

and thus, for $t << \lambda^{-1}$ we can consider that particles move ballistically at speed v_0, while for $t >> \lambda^{-1}$ their motion is characterized by a diffusion coefficient $D = v_0^2\lambda^{-1}$.

2.2 Reaction processes

Our intention is to make a necessary step towards an understanding of phase transitions into absorbing states by studying the dependencies of the equilibrium densities of particles species with motility parameters. Given our goal, any reaction process with an absorbing state serves to our purpose. Prototypical examples of such reaction processes are – using the terminology of epidemics[49] – the Susceptible-Infected-Susceptible (SIS) reaction, which defines the so-called contact process in physics[27–29] or the Susceptible-Infected-Recovered-Susceptible (SIRS) dynamics, which defines a simple spatially extended excitable system, e.g. the Forest-Fire model[27,28]. Note that though here we use terminology of epidemics, many physical systems fall in the same universality class as indicated in[27]. Given that for dilute systems, we expect the SIRS model to behave as the SIS model for fast $R\to S$ transitions, and to recover the SIR model in the absence of such transition. Thus, to remain as general as possible, we choose the SIRS model, whose dynamics is defined by:

$$S + I \xrightarrow{\alpha} 2I, \quad I \xrightarrow{\beta} R, \quad R \xrightarrow{\gamma} S\,, \tag{4}$$

where α, β, and γ are (constant) transition rates. Note that the reaction $S+I\to 2I$ to occur requires a particle of the species "S" and an particle of the species "I" to maintain physical contact for a finite time. We say that two particles are in physical contact whenever the center of mass of these two particles, e.g. $\mathbf{x}$ and $\mathbf{x}'$ are such that $U(\mathbf{x},\mathbf{x}') > 0$. Note that since we are considering active particles that obey an over-damped dynamics, see Eq. (1),

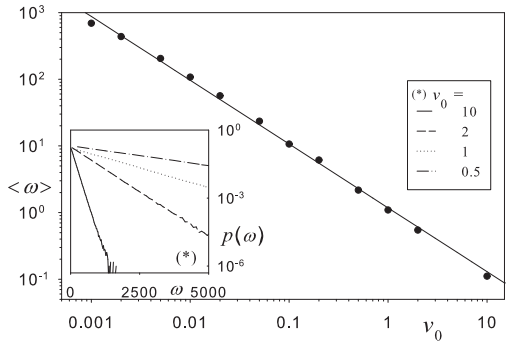

Fig. 2 Collision statistics. Average collision duration time $\langle\omega\rangle$ as function of the active speed v_0. Symbols correspond to simulations, while the solid line is a power-law fit, see Eq. (13). The inset shows that $p(\omega)$ is exponential distributed. The different curves correspond to various values of v_0.

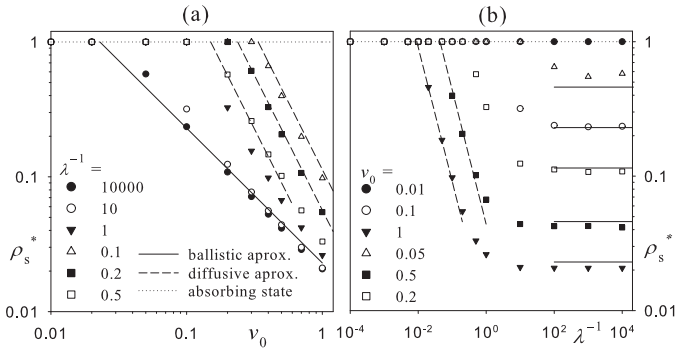

Fig. 3 Instantaneous transmission. (a) ρ_S^* vs. v_0 for various values of λ. (b) ρ_S^* vs. λ^{-1} for various values of v_0. In (a) and (b), symbols correspond to simulations, while solid lines to the ballistic and dashed line to the diffusive approximation. The absorbing state is indicated by the horizontal dotted line.

collisions are not instantaneous and last a finite time; and more importantly, during a collision particles maintain physical contact. In the following, without loss of generality we fix $\beta^{-1} = 200$ and $\gamma^{-1} = 500$ (in arbitrary time units) and vary the reaction rate α since it is the only rate connected to a transition that is affected by particle motion.

3 Mean-field

At higher densities and active speeds, a system of self-propelled disks can undergo a phase separation[23,24]. However, here we use parameters that ensure that the system remains in a gas-like phase, where clusters are small, collisions are mainly binary, and the system is well-mixed. Under these conditions, the temporal evolution of the densities of particle species S, I and R can be described by a mean-field approach of the form:

$$\dot{\rho_S} = \gamma(1-\rho_S-\rho_I) - \psi(v_0,\lambda,\alpha)R(d_0,v_0,\lambda)\rho_I\rho_S\,, \quad (5)$$

$$\dot{\rho_I} = \psi(v_0,\lambda,\alpha)R(d_0,v_0,\lambda)\rho_I\rho_S - \beta\rho_I\,, \quad (6)$$

where the dot denotes time derivative and ρ_S, ρ_I, and ρ_R are normalized densities such that $\rho_S+\rho_I+\rho_R = 1$; the actual densities correspond to $\rho_k d_0$, with $k \in \{S,I,R\}$ and $d_0 = N/L^2$ the (global) density of particles. Note that in deriving Eqs. (5) and (6) we have used that due to particle conservation $\rho_R = 1-(\rho_S+\rho_I)$. For details on the derivation of population mean-field models, see e.g.[49]. It is important to understand that in a standard all-to-all mean-field scheme the expected term in front of $\rho_I\rho_S$ in Eqs. (5) and (6) is α times a constant (i.e. N for $N \gg 1$). However, here due to the active motion of the disks, particles are rarely in contact and when they do it, it is only for a short period of time. The question we pose is then how to effectively renormalize the transition rate $I \to S$ and how such an effective transition rate depends on the motility parameters. To compute an effective transition rate, we need to estimate the rate at which particles meet – let us call this rate the collision frequency and denote it by $R(d_0,v_0,\lambda)$ – and the probability that a reaction $I \to S$ occurs for a random encounter between a particle S and a particle I; let us use the symbol $\psi(v_0,\lambda,\alpha)$ to refer to this probability. In summary, $R(d_0,v_0,\lambda)\psi(v_0,\lambda,\alpha)$ defines the effective transition rate $I \to S$. Now, let us assume we know R and ψ (we estimate both of them below). It is straightforward to verify that Eqs. (5) and (6) have two steady states. One of these states, often referred to as the *absorbing phase*, is given by $\rho_S(t\to\infty) = 1$ and $\rho_I(t\to\infty) = 0$. The other one, called the *active phase*, is given by:

$$\rho_S(t\to\infty) = \rho_S^* = \frac{\beta}{\psi(v_0,\lambda,\alpha)R(d_0,v_0,\lambda)}\,, \quad (7)$$

$$\rho_I(t\to\infty) = \rho_I^* = \frac{\gamma}{\gamma+\beta}\left(1-\rho_S(t\to\infty)\right)\,. \quad (8)$$

Strictly speaking, Eqs. (7) and (8) correspond to the (active) steady states of an infinite system of density d_0. Finite size fluctuations, which we have neglected here, may lead to deviation of mean-field predictions. The linear stability analysis around the absorbing state ($\rho_S = 1$, $\rho_I = 0$) – obtained by inserting $\rho_S = 1-\delta(t)$ and $\rho_I = \delta(t)$ into Eq. (8) and keeping linear terms in δ – provides the following condition (within the mean-field approximation) for the existence of the active phase:

$$\psi(v_0,\lambda,\alpha)R(d_0,v_0,\lambda) > \beta\,. \quad (9)$$

In the following, we provide estimates for $R(d_0,v_0,\lambda)$ and $\psi(v_0,\lambda,\alpha)$.

3.1 Time in between collisions – estimating R

To estimate $R(d_0,v_0,\lambda)$, we consider that there are two clearly distinct regimes that we can identify by constructing a dimensionless quantity (l_{ball}/l_ρ) that results from the ratio between two characteristic length scales in the system: the characteristic distance l_ρ in between particles – neglecting clustering effects and assuming a homogeneous distribution of particles – which is given by $l_\rho = 1/\sqrt{d_0}$, and the typical distance l_{ball} that particles move in straight line (i.e. the typical distance in between two tumbling events). Since the typical time in between tumbling events is λ^{-1}, then $l_{ball} = v_0\lambda^{-1}$. Now, we are in condition of defining the *ballis-*

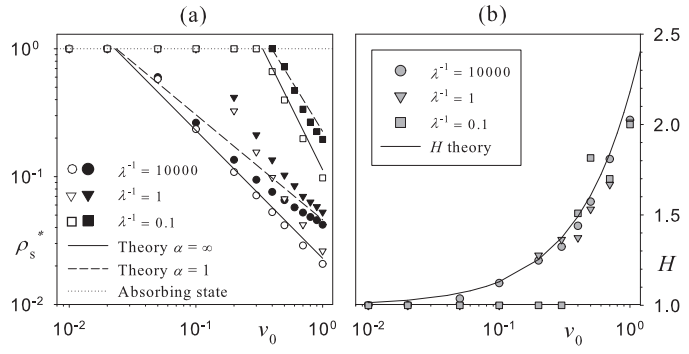

Fig. 4 Finite transmission - (a) $\rho_S(t \to \infty)$ vs. v_0 for various λ values. Open symbols correspond to simulations with $\alpha \to \infty$, while solid symbols to $\alpha = 1$. The solid and dashed curve correspond to the mean-field approximation for $\alpha \to \infty$ and $\alpha = 1$, respectively, in both ballistic and diffusive approximation. (b) $H = \rho_S^*(\alpha)/\rho_S^*(\infty)$ vs. v_0 for various λ values. Simulations (symbols) follow the mean-field prediction (solid curve) as soon as the system moves into the active phase.

tic and *diffusive* spreading regimes. We call ballistic spreading, the regime in which we can ensure that in between collisions, active particles move ballistically, i.e. in straight lines. The condition for this regime is given by:

$$l_{ball}/l_\rho = v_0 \lambda^{-1} \sqrt{d_0} \gg 1 \,. \tag{10}$$

Under this condition, we can make use of kinetic gas theory[50] and approximate $R(d_0, v_0, \lambda)$ as:

$$R(\rho, v_0, \lambda) \sim v_0 \sigma_0 d_0 \,, \tag{11}$$

where $\sigma_0 = 4r$ is the scattering cross section of particles (v_0 and d_0 were defined above). The diffusive spreading regime corresponds to the opposite limite: $l_{ball}/l_\rho \ll 1$. In this regime, active particles perform several tumbling events in between collisions. This implies that the time in between collisions is much larger than λ^{-1}, which according to Eq. (3) means that the active particles are deep inside the diffusive regime. In other words, the time in between collisions is dictated by a diffusive process characterized by a diffusion constant D, whose expression was given above after Eq. (3). To estimate the time in between collisions – let us refer to it as τ – we consider that the centers of mass of two neighboring self-propelled disks are separated an average distance $1/\sqrt{d_0}$ and that the average distance the disks have to travel to collide is $1/\sqrt{d_0} - 2r$, since the disks have a radius r. Then, under the assumption we are in the diffusive regime, we expect τ to be such that $\left(1/\sqrt{d_0} - 2r\right)^2 \simeq D\tau$. Thus, the collision frequency R, which is the inverse of τ, takes the form:

$$R(d_0, v_0, \lambda) \sim v_0^2 \lambda^{-1} \left(\frac{1}{\sqrt{d_0}} - 2r \right)^{-2} . \tag{12}$$

Note that the above expression is only an approximation. A rigorous calculation of the collision frequency would require to solve a first passage time problem; for details see[28,51].

3.2 Collision duration – estimating ψ

A collision between two particles is a relatively slow process in which particles stay in contact – understanding by this that the potential energy U between the two particles is larger than 0 – for a finite time ω. By looking at histograms of ω in simulations, we learn that ω is exponentially distributed – meaning that $p(\omega) = \exp(-\omega/\langle\omega\rangle)/\langle\omega\rangle$ –, see inset in Fig. 2. Furthermore, by performing a systematic study of $\langle\omega\rangle$ vs. v_0, Fig. 2, we find that $\langle\omega\rangle$ follows a power-law with v_0:

$$\langle\omega\rangle = k\, v_0^{-\xi} \,, \tag{13}$$

with $k = 1.18$ and $\xi = 0.957$ for λ^{-1} larger than r/v_0 *. Knowing the statistics of ω, now we can focus on obtaining an estimate for the probability that, during a collision event of duration ω between a particle I and a particle S, a reaction $S + I \to 2I$ occurs. We make use of the fact that the reaction is given by a simple Poissonian process[52], which let us compute the probability that a reaction takes place in the time interval ω as $1 - e^{-\omega\alpha}$, under the assumption that the initial particle I does not transition to R in this time interval. The next step to estimate ψ is to make an average over all possible collision durations ω – that we know is distributed exponentially as indicated above – to express ψ as:

$$\psi(v_0, \lambda, \alpha) = \int_0^\infty d\omega\, p(\omega) \left(1 - e^{-\omega\alpha}\right) = \frac{\alpha\langle\omega\rangle}{1 + \alpha\langle\omega\rangle} \,. \tag{14}$$

Thus, inserting Eq. (13) into Eq. (14), we find that $\psi = (1 + k^{-1}\alpha^{-1} v_0^{\xi})^{-1}$.

4 Comparison with simulations

Let us start by analyzing an infinitely fast reaction rate α, which let us take the limit $\alpha \to \infty$ in Eq. (14) and express $\psi = 1$. The prediction is that for $l_{ball}/l_\rho \gg 1$, by inserting Eq. (11) into Eq. (7), we find $\rho_S^* \sim v_0^{-1}$, solid curve in Fig. 3(a), while by inserting Eq. (12) into Eq. (7), we obtain $\rho_S^* \sim \lambda\, v_0^{-2}$, dashed curves in Fig. 3(a). In summary, there are at least two scalings of ρ_S^* with v_0, and a crossover between these two scalings at $l_{ball}/l_\rho \simeq 1$. Fixing v_0, the set of mean-field approximations detailed above predicts that at large enough tumbling frequencies λ such that $l_{ball}/l_\rho \ll 1$, $\rho_S^* \propto \lambda$, dashed curves in Fig. 3(b). As λ is decreased, the system should cross $l_{ball}/l_\rho = 1$ and ρ_S^* becomes independent of λ, as confirmed by the horizontal solid lines in Fig. 3(b).

Now, we move to finite reaction rates α, where the approximations given above suggest that the spreading dynamics is strongly affected by the average collision duration $\langle\omega\rangle$ through Eq. (14). The predictions are now $\rho_S^* \sim v_0^{\xi-1}$ for the ballistic regime, that consists of inserting Eq. (11) and Eq. (14) into Eq. (7), and $\rho_S^* \sim \lambda\, v_0^{\xi-2}$ for the diffusive regime, obtained by inserting Eq. (12) and Eq. (14) into Eq. (7) †. Fig. 4(a) shows a direct comparison between the prediction for finite (dashed curves) and infinitely fast reaction rates α (solid curves). In order to get a direct understanding of the role of the probability ψ, we plot in Fig. 4(b)

* For λ^{-1} smaller or equal to r/v_0, we find that $\xi \sim 0.5$. This regime is out of the scope of the current study and will be analyzed elsewhere.

† In both cases, the factorization was performed assuming $\alpha k < v_0^{\xi}$.

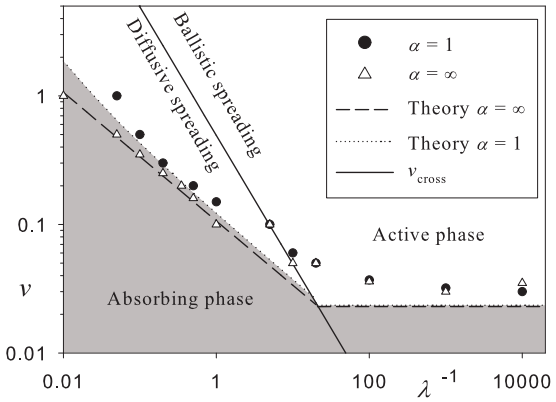

Fig. 5 Phase diagram v vs λ^{-1}. Symbols correspond to the absorbing-active boundary as found in simulations. Dashed and dotted lines correspond to the critical point (λ_c^{-1}, v_c) predicted by the mean-field approximation for $\alpha \to \infty$ and $\alpha = 1$, respectively. The solid line, v_{cross}, indicates the crossover between ballistic and diffusive spreading.

$H = \rho_S^*(\alpha)/\rho_S^*(\alpha \to \infty)$ (let us recall that $\rho_S^*(\alpha \to \infty) \sim v_0^{-1}$ and $\rho_S^*(\alpha \to \infty) \sim \lambda\, v_0^{-2}$ for the ballistic and diffusive regime, respectively). Thus, according to the approximations developed in the previous sections, for both regimes, i.e. ballistic and diffusive, $H \sim (1 + k^{-1}\, \alpha^{-1}\, v_0^{\xi})$, see solid curve in Fig. 4(b).

In the following, we look for the critical active speed v_c (and tumbling rate λ_c) above (below) which the active phase should be observed. We are particularly interested in knowing, given a set of parameters α, β, γ, and d_0, the behavior of v_c with the tumbling rate λ. Inserting Eq. (11) and Eq. (14) into Eq. (7), and by requesting $\rho_S^* = 1$, we derive a condition for v_c which does not depend on λ; see horizontal lines in Fig.5. Similarly, by inserting Eq. (12) and Eq. (14) into Eq. (7), and under the same condition, we find that v_c is solution of $v_c^2 - q\lambda\varepsilon v_c^{\xi} = q\lambda$, where $q = \beta(1/\sqrt{d_0} - 2r)^2$ and $\varepsilon = 1/\alpha$. In order to obtain a close expression for v_c, we assume that ε is small and $\xi = 1 + \delta$, with $|\delta| \ll 1$, which leads to:

$$v_c = \frac{\varepsilon q \lambda}{2} + \left[q\lambda \left(1 + \frac{\varepsilon^2 q \lambda}{4} \right) \right]^{-1/2} \tag{15}$$

where terms proportional to $\varepsilon\delta$ have been neglected. For infinitely fast reactions, $\varepsilon \to 0$, and $v_c \propto \lambda^{1/2}$. Note that this result is independent of δ. For large, but finite reaction rates, Eq. (15) provides a good estimate of v_c as shown in Fig. 5. Using Eq. (10) and the fact that the ballistic and diffusive approximation for ρ_S^* coincide at the crossover point, we find $v_{cross}(\lambda_c)$, the solid curve in Fig. 5.

5 Conclusions

We have studied, combining individual-based simulations and mean-field arguments, the dependency of the equilibrium densities of particle species with motility parameters in an active system consisting of self-propelled disks. Importantly, we consider a reaction process with an absorbing and active state. For a finite reaction rate α, we found that there are two distinct regimes in the active phase with the active speed v_0 and tumbling frequency λ that lead to steady state densities $\rho_S^* \propto v_0^{\xi-1}$ and $\rho_S^* \propto \lambda v_0^{\xi-2}$ for the ballistic and diffusive regime, respectively. For a given set of reaction rates α, β, and γ, and density d_0, we have been able to compute the phase-diagram in terms of motility parameters, namely v_c and λ_c, that separates the absorbing and active phase. These results were obtained from a combination of stochastic simulations of the microscopic dynamics and mean-field arguments. It is important to stress that the developed mean-field arguments include information on the spatial dynamics of the self-propelled disks. Moreover, the results here derived cannot be obtained by a classical reaction-diffusion process as done in [49], since these approaches decouple particle motility and effective reaction rates and assume that particle transport is always diffusive. A word of warning: the here derived arguments neglect spatial correlations among the particle species. At higher densities, lower dimensions, and/or close to the critical point, deviations between the derived mean-field arguments and simulations are expected, and correlation and fluctuations should be taken into account in order to obtain an accurate description of the system dynamics along the lines explained in [53] that makes used of the formalism developed in [54].

Here, we have shown that the (transient) behavior of the active particles in between collisions plays a key role to understand the equilibrium densities of particle species. While here we considered only ballistic and diffusive regimes, we can imagine a more general scenario where $\langle \mathbf{x}^2 \rangle \propto t^{\chi}$ with $1 \leq \chi \leq 2$ that we expect to lead to different scalings of the equilibrium densities with active speed v_0 and tumbling frequency λ. Importantly, the presence of different transport regimes in systems of active particles suggests that phase transitions into an absorbing state do not necessarily fall into the directed percolation class or related universality classes for active systems [27,29]. Understanding in which universality class fall "reactive" active systems with an absorbing state remains a fundamental, challenging question that can only be addressed by combining large-scale simulations and renormalization group techniques, which we hope will be the subject of future works.

The simple, but fundamental results reported in this study represent a necessary first step to a better understanding on the spreading of information/signaling among actively moving units, an issue of key importance in the context of reaction processes and diseases [32,40–42], synchronization among moving oscillators [55–59], organization of self-propelled particles into collective motion [11,12,14–16,60], as well as several technological and biomedical applications involving moving entities [61,62].

Conflicts of interest

There are no conflicts of interests to declare.

Acknowledgements

F. P. was supported by the Agence Nationale de la Recherche via project BactPhys, Grant No. ANR-15- CE30-0002-01.

Notes and references

1 H. Zhang, A. Be'er, E.-L. Florin and H. Swinney, *Proc. Natl. Acad. Sci. USA*, 2010, **107**, 13526.

2 L. H. Cisneros, J. O. Kessler, S. Ganguly and R. E. Goldstein, *Phys. Rev. E*, 2011, **83**, 061907.
3 F. Peruani, J. Starruss, V. Jakovlievic, L. Søgaard-Anderson, A. Deutsch and M. Bär, *Phys. Rev. Lett.*, 2012, **108**, 098102.
4 M. Ballerini, N. Cabibbo, R. Candelier, A. Cavagna, E. Cisbani, I. Giardina, V. Lecompte, A. Orlandi, G. Parisi, A. Procaccini, M. Viale and V. Zdravkovic, *Proc. Natl. Acad. Sci. USA*, 2008, **105**, 1232.
5 F. Ginelli, F. Peruani, M.-H. Pillot, H. Chaté, G. Theraulaz and R. Bon, *Proc. Nat. Acad. Sci.*, 2015, **112**, 12729–12734.
6 J. R. Howse, R. A. L. Jones, A. Ryan, T. Gough, R. Vafabakhsh and R. Golestanian, *Phys. Rev. E*, 2007, **99**, 048102.
7 W. E. Uspal, M. N. Popescu, S. Dietrich and M. Tasinkevych, *Soft Matter*, 2015, **11**, 434.
8 J. Deseigne, O. Dauchot and H. Chaté, *Phys. Rev. Lett.*, 2010, **105**, 098001.
9 A. Bricard, J.-B. Caussin, D. Debasish, C. Savoie, V. Chikkadi, K. Shitara, O. Chepizhko, F. Peruani, D. Saintillan and D. Bartolo, *Nature Comm.*, 2015, **6**, 7470.
10 A. Kaiser, A. Snezhko and I. S. Aranson, *Science advances*, 2017, **3**, e1601469.
11 T. Vicsek and A. Zafeiris, *Physics Reports*, 2012, **517**, 71–140.
12 M. C. Marchetti, J. F. Joanny, S. Ramaswamy, T. B. Liverpool, M. R. J. Prost and R. A. Simha, *Rev. Mod. Phys.*, 2013, **85**, 1143.
13 C. Bechinger, R. D. Leonardo, H. Loewen, C. R. Reichhardt, G. Volpe and G. Volpe, *Rev. Mod. Phys.*, 2016, **88**, 045006.
14 T. Vicsek, A. Czirók, E. Ben-Jacob, I. Cohen and O. Shochet, *Phys. Rev. Lett.*, 1995, **75**, 1226.
15 J. Toner and Y. Tu, *Phys. Rev. Lett.*, 1995, **75**, 4326.
16 F. Ginelli, F. Peruani, M. Bär and H. Chaté, *Phys. Rev. Lett.*, 2010, **104**, 184502.
17 D. Nishiguchi, K. H. Nagai, H. Chaté and M. Sano, *Phys. Rev. E*, 2017, **95**, 020601.
18 O. Chepizhko and F. Peruani, *Phys. Rev. Lett.*, 2013, **111**, 160604.
19 F. Peruani and I. Aranson, *Phys. Rev. Lett.*, 2018, **120**, 238101.
20 S. Ramaswamy, *J. Stat. Mech.*, 2017, 054002.
21 F. Peruani, A. Deutsch and M. Bar, *Phys. Rev. E*, 2006, **74**, 030904(R).
22 Y. Yang, V. Marceau and G. Gompper, *Phys. Rev. E*, 2010, **82**, 031904.
23 Y. Fily and M. C. Marchetti, *Phys. Rev. Lett.*, 2012, **108**, 235702.
24 J. Bialké, H. Löwen and T. Speck, *Europhys. Lett.*, 2013, **103**, 30008.
25 I. Buttinoni, J. Bialké, F. Kümmel, H. Löwen, C. Bechinger and T. Speck, *Phys. Rev. Lett.*, 2013, **110**, 238301.
26 M. Enculescu and H. Stark, *Phys. Rev. Lett.*, 2011, **107**, 058301.
27 H. Hinrichsen, *Advances in physics*, 2000, **49**, 815–958.
28 P. L. Krapivsky, S. Redner and E. Ben-Naim, *A kinetic view of statistical physics*, Cambridge University Press, 2010.
29 J. Marro and R. Dickman, *Nonequilibrium phase transition in lattice models*, Cambridge University Press, Cambridge, 1999.
30 A. F. Taylor, M. R. Tinsley, F. Wang, Z. Huang and K. Showalter, *Science*, 2009, **323**, 614–617.
31 M. R. Tinsley, A. F. Taylor, Z. Huang and K. Showalter, *Phys. Rev. Lett.*, 2009, **102**, 158301.
32 T. Reichenbach, M. Mobilia and E. Frey, *Nature (London)*, 2007, **448**, 1046–1049.
33 T. Reichenbach, M. Mobilia and E. Frey, *Phys. Rev. Lett.*, 2007, **99**, 238105.
34 M. Kuperman and G. Abramson, *Phys. Rev. Lett.*, 2001, **86**, 2909.
35 M. Boguna, R. Pastor-Satorras and A. Vespignani, *Phys. Rev. Lett.*, 2003, **90**, 028701.
36 V. Colizza, R. Pastor-Satorras and A. Vespignani, *Nature Physics*, 2007, **3**, 276.
37 L. Hufnagel, D. Brockmann and T. Geisel, *Proc. Natl. Acad. Sci. USA*, 2004, **101**, 15124.
38 M. Gonzalez and H. Herrmann, *Physica A*, 2004, **340**, 741.
39 O. Miramontes and B. Luque, *Physica D*, 2002, **379**, 168.
40 M. G. Weinbauer and M. G. Höfle, *Aquat. Microb. Ecol.*, 1998, **15**, 103.
41 E. Beretta and Y. Kuang, *Math. Biosci.*, 1998, **149**, 57.
42 M. Dworking and D. Kaiser, *Myxobacteria II*, American Society of Microbiology, Washington, DC, 1993.
43 M. Gonzalez, P. Lind and H. Herrmann, *Phys. Rev. Lett.*, 2006, **96**, 088702.
44 G. R. Terranova, J. A. Revelli and G. J. Sibona, *Europhys. Lett.*, 2014, **105**, 30007.
45 N. C. Clementi, J. A. Revelli and G. J. Sibona, *Phys. Rev. E*, 2015, **92**, 012816.
46 F. Peruani and G. J. Sibona, *Phys. Rev. Lett.*, 2008, **100**, 168103.
47 H. C. Berg, *Random walks in biology*, Princeton University Press, 1993.
48 M. Cates and J. Tailleur, *Europhys. Lett.*, 2013, **101**, 20010.
49 J. Murray, *Mathematical Biology*, Springer-Verlag, New York, 1989.
50 F. Reif, *Fundamentals of statistical and thermal physics*, Waveland Press, 2009.
51 S. Redner, *A guide to first-passage processes*, Cambridge University Press, 2001.
52 N. G. Van Kampen, *Stochastic processes in physics and chemistry*, Elsevier, 1992, vol. 1.
53 F. Peruani and C. F. Lee, *Europhys. Lett.*, 2013, **102**, 58001.
54 L. Peliti, *J. Phys. (Paris)*, 1985, **46**, 1469.
55 J. D. Skufca and E. M. Bollt, *Math. Biosci. Eng.*, 2004, **1**, 347.
56 M. Frasca, A. Buscarino, A. Rizzo, L. Fortuna and S. Boccaletti, *Phys. Rev. Lett.*, 2008, **100**, 044102.
57 F. Peruani, E. Nicola and L. Morelli, *New J. Phys.*, 2010, **12**, 093029.
58 N. Fujiwara, J. Kurths and A. Díaz-Guilera, *Phys. Rev. E*, 2011, **83**, 025101.
59 R. Großmann, F. Peruani and M. Bär, *Phys. Rev. E*, 2016, **93**,

040102.
60 L. Barberis and F. Peruani, *Phys. Rev. Lett.*, 2016, **117**, 248001.
61 F. G. Woodhouse and J. Dunkel, *Nature Communications*, 2017, **8**, 15169.
62 M. O. Din, T. Danino, A. Prindle, M. Skalak, J. Selimkhanov, K. Allen, E. Julio, E. Atolia, L. S. Tsimring, S. N. Bhatia and J. Hasty, *Nature*, 2016, **536**, 81.